Indian Journal of Experimental Biology
Vol. 64, October 2026, pp. 932-943
DOI: 10.56042/ijeb.v64i10.31660

Pathological and ultrastructural changes of Adrenal Cortex and their association with Adrenal insufficiency in a Rat Model of Severe Acute Pancreatitis

Lilei Liu[1*], Xingwen Zhang[2], Xiang Li[1], Jing Xu[2], Yanfang Pei[1], Maiying Fan[1], Fang Yu[1], Xiangying Wang[3] & Xiaotong Han[1*]

[1]Department I; [2]Department III; and [3]Department of Critical Care Medicine, Hunan Provincial People's Hospital First Affiliated Hospital of Hunan Normal University, Changsha 410000, Hunan Province, China

Received 18 May 2026; revised 24 July 2026

Acute pancreatitis is an acute inflammatory disease characterized by pancreatic tissue self digestion, which leads to local pancreatic injury or systemic inflammatory response. The mortality of acute pancreatitis is high, up to 36-50%, which seriously threatens the life safety of patients. During the development of SAP, multiple extra pancreatic organs may be involved in the early stage, and the kidney is one of the most frequently affected organs. Early detection of renal function, early diagnosis and treatment of SAP can reduce the mortality. Here, we have explored the pathological and ultrastructural changes of adrenal gland in severe acute pancreatitis (SAP) as well as the mechanism and treatment of SAP affecting adrenal function. The results showed that the mortality of so group was 3.6% and that of SAP group was 27%. The injury and secretion function of adrenocortical cells were decreased in SAP. Intracellular calcium as well as the disturbance of pancreatic microcirculation plays an important role in the occurrence and development of SAP. Hence, the level of calcium ions helps in predicting the prognosis in SAP patients.

Keywords: Adrenal Pathology, Microcirculation Disturbance, Severe Acute Pancreatitis

Introduction

Acute pancreatitis (AP) is a highly prevalent acute abdominal condition, with its severe form (SAP) posing significant clinical challenges due to its critical progression and numerous complications[1]. Early-stage systemic inflammatory response syndrome (SIRS) and mid-to-late stage multiple organ dysfunction syndromes (MODS) are the primary causes of mortality in such cases. During SAP progression, extra-pancreatic organ involvement is common. While the kidney, as a classic target organ, has been extensively studied, the pathological changes and mechanisms of the adrenal gland, another crucial stress-regulating organ, have not yet been systematically investigated[2].

Severe acute pancreatitis (SAP) is a serious inflammatory condition in which pancreatic enzymes become prematurely activated, causing self-digestion of pancreatic tissue, inflammation, edema, hemorrhage, and even organ failure. Common causes include gallstones, alcohol abuse, infections, trauma, and pancreatic duct obstruction. SAP triggers a strong inflammatory response through cytokines and activated enzymes, leading to systemic inflammatory response syndrome (SIRS) and multiple organ dysfunction syndromes (MODS). Renal injury occurs due to microcirculatory disturbances, ischemia-reperfusion injury, endothelial damage, and inflammatory mediators that impair kidney filtration and oxygen supply. Early treatment mainly focuses on aggressive fluid resuscitation, infection control, and maintaining hemodynamic stability.

The adrenal gland is a vital endocrine organ that maintains physiological homeostasis and enhances the body's stress response through hormones produced by the adrenal cortex. In SAP, adrenal insufficiency (AI) is difficult to diagnose because its symptoms are often nonspecific or masked by the primary disease. Current diagnostic methods, including serum cortisol measurement and adrenocorticotropic hormone (ACTH) stimulation tests, have limited accuracy, making the diagnosis and management of AI highly controversial.

Current studies have confirmed that SAP patients often exhibit adrenal insufficiency (AI), characterized

*Correspondence:
E-mail: liulileibelian@163.com

Abbreviations: ACTH: Adrenocorticotropic hormone; AI: Adrenal insufficiency; AKI: Acute kidney injury; ALB: Albumin; AP: Acute pancreatitis.

by abnormal corticosteroid secretion, which is closely associated with worsened prognosis and increased mortality[3,4]. However, existing research on SAP-associated AI has notable limitations. Most studies focus on serum hormone level fluctuations while lacking direct histological observations of adrenal tissue. Investigations into adrenal ultrastructural alterations (e.g., organelle damage and intercellular junction disruption) remain virtually absent; despite these microscopic changes constituting the structural basis of functional impairment[5-7]. Furthermore, serum cortisol measurement and ACTH stimulation tests cannot reliably differentiate between primary adrenal injury and hypothalamic-pituitary-adrenal (HPA) axis dysregulation, leading to therapeutic dilemmas[8].

A thorough literature review reveals that SAP pathological mechanisms have been predominantly investigated in relation to pancreatic microcirculatory dysfunction, intracellular calcium overload, and cytokine storms, yet their specific effects on adrenal tissue remain poorly understood[9,10]. While pancreatic microcirculatory disturbances may affect distant organ perfusion through systemic inflammation, the unique vascular architecture of the adrenal gland (e.g., abundant sinusoids and hypoxia sensitivity) suggests potentially distinct injury patterns compared with other organs. Similarly, although intracellular calcium dysregulation represents a core pathogenic mechanism in SAP, its potential role in adrenal cortical cell dysfunction lacks experimental validation[11,12]. Moreover, despite reports of SAP-induced ultrastructural changes in multiple organs, specific damage to critical organelles such as mitochondria and the endoplasmic reticulum in adrenal cortical cells has not been systematically documented.

While previous studies have largely focused on SAP-induced pancreatic damage and dysfunction of organs such as the lungs and kidneys, systematic research on the relationship between adrenal cortical morphology, particularly ultrastructural changes, and adrenal insufficiency is lacking. The key pathological mechanisms and potential predictive indicators of SAP-induced adrenal injury have not been clearly defined. Therefore, we used a rat SAP model to perform histological and ultrastructural examination of the adrenal cortex together with measurement of serum cortisol and ACTH levels. We also evaluated potential predictive indicators, including C-reactive protein (CRP) and APACHE II scores, to investigate the mechanisms of SAP-associated adrenal dysfunction and provide an experimental basis for early clinical intervention.

The specific objectives of this study are: (i) To determine whether SAP induces structural damage in adrenal cortical cells during disease progression; (ii) To assess the correlation between adrenal injury severity and systemic indicators such as serum amylase, albumin, and calcium levels; and (iii) To explore the potential mechanistic link between adrenal morphological changes and the development of adrenal insufficiency (AI) in SAP.

Materials and Methods

Experimental object and model preparation

This experimental protocol was approved by the Institutional Animal Care and Use Committee (Approval No.: 24-2D) and strictly adhered to ethical guidelines for laboratory animals. This manuscript was prepared without the use of AI tools.

Thirty-six SPF-grade male Wistar rats (200-250 g) were selected. The sample size was determined based on effect size analysis from previous SAP studies, considering variations in adrenal pathological indicators from preliminary experiments, anticipated intergroup differences, and potential mortality during model establishment. Each group was allocated 18 rats to ensure statistically adequate sample sizes at all time points. Rats were randomly divided into a sham operation group (SO) and a SAP group, with 18 rats in each group. Each group was further subdivided into three observation time points (3, 12 and, 24 h), with 6 to 7 rats at each time point. As the sample size at each time point was small ($n \leq 10$), the data were expressed as median (interquartile range) [median (IQR)]. These time points were selected according to SAP pathological progression characteristics: 3 h represents the early disease stage featuring pancreatic autodigestion initiation and systemic inflammatory response onset; 12 h corresponds to the inflammatory progression phase with massive proinflammatory cytokine release and emerging extra-pancreatic organ involvement; 24 h represents the multiple organ injury phase, coinciding with potential AI in SAP, thereby enabling dynamic observation of adrenal changes throughout disease progression. All rats were housed in an SPF-level animal facility. The ambient temperature was controlled at 22±2°C, with a relative humidity of 55±5%. A 12 h light/dark cycle (light period: 07:00-19:00) was maintained. Standard rodent

chow (purchased from Beijing HuaFuKang Biological Technology Co., Ltd.) and sterile drinking water were provided *ad libitum*. Following one week of acclimatization, experiments were conducted.

All rats underwent 12 h fasting and 4 h water deprivation before surgery. Anesthesia was induced by intraperitoneal injection of 10% chloral hydrate (3 mL/kg). Under aseptic conditions, the SAP group underwent duodenal mesentery-free border puncture followed by retrograde injection of 5% sodium taurocholate solution (1 mL/kg) into the pancreaticobiliary duct at a constant rate. The main pancreatic duct was clamped for 5 min, with successful model establishment confirmed by observable pancreatic hemorrhage and edema before abdominal closure. The SO group received only duodenal and pancreatic manipulation before closure. Postoperatively, both groups received subcutaneous normal saline (10 mL/kg) for fluid maintenance.

The sample size of the present study was calculated with the semi-quantitative score for adrenal cortical injury as the primary outcome measure, and the analytical process was designed based on a general statistical model. For the purpose of sample size estimation, one-way analysis of variance (ANOVA) was adopted for continuous data, and the Kruskal-Wallis H test was used for ordinal data to assess the overall differences among groups and at different time points. Based on the pilot study data, the standard deviation of this indicator was 0.32 in both the SAP group and the SO group, and the expected minimal clinically meaningful difference (effect size) between groups was 0.65. A two-tailed test with $\alpha=0.05$ and a test power $(1-\beta)=0.85$ were set. The sample size calculation formula ($n=2\times(Z\alpha/2 + Z1-\beta)^2\times s^2/\delta^2$) was applied, and the minimum required sample size of 14 rats per group was obtained (Note: 14 rats was the standard for the total sample size per group). Considering the potential mortality rate (estimated 10-15%) and the risk of sample loss during the establishment of the SAP model, 18 rats were ultimately included in each group to ensure that the total effective sample size met or exceeded the estimated standard. The rats were evenly divided into three observation time points (3, 12 and 24 h), with 6–7 rats per group at each time point. Given the small-sample characteristic of $n < 10$ per single time point in this study, all continuous variables were first tested for normality and homogeneity of variance across subgroups (each time point × each group). Variables meeting the test criteria were analyzed using parametric tests, while those not meeting the criteria were directly analyzed using nonparametric tests. Additionally, Bootstrap resampling (1,000 times) was performed to verify the robustness of all statistical results, thereby addressing the insufficient power of parametric tests in small samples. It should be noted that, although the sample size at a single time point was lower than the total sample size estimation standard, it still met the basic requirements for analyzing overall differences between groups and across different time points. Meanwhile, it should be objectively pointed out that the relatively limited sample size at a single time point might result in low power for some statistical tests and an inherent risk of Type II error. Future studies could further optimize the study design to ensure that the total sample size per group strictly met the standard and was rationally allocated to each time point, thereby further verifying the reliability and stability of the study results.

Ultrastructural observation and statistical treatment of adrenal cortex

The left adrenal tissues of rats in the two groups were fixed with 2.5% glutaraldehyde and 1% osmium acid, embedded in EPON 812 embedding machine, sliced with lkb-v ultra-thin section machine, stained with uranium acetate and lead citrate, and observed under H-300 transmission electron microscope. In addition to morphological observations, AI was comprehensively assessed through the following indicators. Serum cortisol level measurement was conducted. Blood samples were collected from the abdominal aorta at each time point, centrifuged (3000 rpm, 10 min) to separate serum, and cortisol concentrations were determined by enzyme-linked immunosorbent assay (ELISA) in strict accordance with the kit instructions. ACTH level measurement was conducted. ACTH concentrations were measured in the same serum samples using ELISA. The cortisol-to-ACTH ratio was analyzed to evaluate adrenal responsiveness to pituitary regulation, thereby determining the presence and severity of AI.

Adrenal cortical ultrastructural damage was quantified using a grading/scoring system. Based on the degree of morphological abnormality in mitochondria, endoplasmic reticulum, lipid droplets, and the nucleus, scores from 0 to 3 were assigned (Grade 0: No abnormality; Grade 1: Mild abnormality; Grade 2: Moderate abnormality; Grade 3: Severe abnormality). The average score for each indicator ($\bar{x}_1$) and the total damage score ($\bar{x}_2$ =

(mitochondrial damage score + ER dilation score + lipid droplet depletion score + nuclear abnormality score)/4) were calculated. Inter-observer scoring consistency was verified using the Intraclass Correlation Coefficient (ICC = 0.92, *P <0.001*), ensuring result reliability.

The serum cortisol ELISA detection kit was purchased from Shanghai Enzyme-linked Biotechnology Co., Ltd. The adrenocorticotropic hormone (ACTH) ELISA detection kit was purchased from R&D Systems, Inc. (USA). 2.5% glutaraldehyde fixative, 1% osmium tetroxide fixative, epoxy resin EPON 812, uranyl acetate, and lead citrate were all purchased from Sigma-Aldrich (USA). Other chemical reagents (e.g., saline, absolute ethanol) were domestically produced analytical grade, purchased from Sinopharm Chemical Reagent Co., Ltd.

The analysis was performed using SPSS 13.0 software. Normality and homogeneity of variance tests were first conducted on the measurement data for each subgroup (group × time point). Data meeting the test criteria were expressed as mean ± standard deviation, and a one-way ANOVA overall model was established. If the overall difference was statistically significant (P <0.05), post hoc tests (Tukey's method) were used to analyze specific differences between groups and across different time points. Data not meeting the test criteria were expressed as median (interquartile range) and analyzed using nonparametric tests. All parametric test results were validated for robustness through Bootstrap resampling (1000 iterations). A *P*-value less than 0.05 was considered statistically significant. The equation of mean and standard deviation is expressed as follows:

$$\mu = A_n = \frac{a_1 + a_2 + a_3 + ... + a_n}{n} \quad \ldots (1)$$

$$\sigma = \sqrt{\frac{1}{N}\sum_{i=1}^{N}(x_i - \mu)^2} \quad \ldots (2)$$

Histopathological examination of pancreatic and adrenal tissues

For pancreatic tissue, pancreatic specimens were fixed in 10% neutral buffered formalin for 24 h, paraffin-embedded, and sectioned (4 μm thickness) for hematoxylin-eosin (HE) staining. Pancreatic injury was assessed using Schmidt scoring system comprising four parameters: edema (0-2 points), hemorrhage (0-2 points), necrosis (0-4 points), and inflammatory infiltration (0-2 points), with total scores ranging from 0 to 10 (higher scores indicating more severe injury).

For adrenal tissue, left adrenal glands were fixed in 10% neutral buffered formalin, paraffin-embedded, and sectioned (4 μm thickness) for HE staining. Adrenal cortical injury was semi-quantitatively graded as: Grade 0 (no injury): intact cortical structure without edema, hemorrhage or inflammatory infiltration; Grade 1 (mild): <30% cortical involvement with mild edema and sinusoid dilation, without significant hemorrhage; Grade 2 (moderate): 30-60% cortical involvement with marked edema, erythrocyte stasis in sinusoids, and mild inflammatory infiltration; Grade 3 (severe): >60% cortical involvement with cellular degeneration/necrosis, patchy hemorrhage, and extensive inflammatory infiltration.

Five randomly selected fields per sample were independently evaluated by two pathologists in a blinded manner, with mean scores calculated.

Statistical Analysis

Statistical analysis was performed using SPSS 26.0 and PASS 15.0 software. The specific tools and their applications are described as follows: The normality of continuous variables (serum amylase, cortisol, ACTH, etc.) was assessed using the Shapiro-Wilk test, with the test units being each subgroup (i.e., SO groups 3, 12 & 24 h and SAP groups 3, 12 & 24 h), rather than the combined groups. Homogeneity of variances was verified using Levene's test, with the same test units as those for the normality test. The following strategies were adopted for inter-group comparisons: For comparisons between groups at a single time point: Independent samples t-tests were used for continuous variables that met both normality and homogeneity of variances; Welch's corrected *t*-tests were used for those that met normality but not homogeneity of variances; Mann-Whitney U tests were used for continuous variables with non-normal distributions and for Likert-scale ordinal categorical variables (semi-quantitative scores of adrenal cortex injury, ultrastructural injury grades). For trend comparisons between different time points within groups: Repeated measures ANOVA was used for continuous variables that met both normality and homogeneity of variances; otherwise, the Kruskal-Wallis H test was used. For all parameter test results from small samples with n <10, robustness was verified via Bootstrap resampling (1000 iterations). Statistical significance was only confirmed when the

resampling results were consistent with the original test results. The annotation standard for *P*-values in all statistical tests was as follows: $P < 0.001$ was set as the lowest annotation threshold, and no $P < 0.001$ was annotated. Measurement data were expressed as median (interquartile range) [M (IQR)] when $n \leq 10$, and as mean ± standard deviation ($\bar{x} \pm s$) when $n > 10$.Non-normally distributed continuous variables and Likert-scale ordinal categorical variables (semi-quantitative adrenal cortical injury scores, ultrastructural damage grading) were analyzed using the Mann-Whitney U test; intra-group trends across multiple time points were analyzed using the Kruskal-Wallis H test; The chi-square test was used to analyze categorical variables when the following two conditions were met simultaneously: (i) the total sample size was no less than 40; (ii) all expected frequencies in the contingency table were no less than 5, so as to ensure the reliability of the test results. Fisher's exact test was adopted if either of the following conditions was satisfied: 1) the total sample size was less than 40; and (iii) any expected frequency in the contingency table was less than 5 (including less than 1), so as to avoid analytical bias caused by sparse data. Mortality in this study was a binary categorical variable, with a total sample size of 42 and all expected frequencies in the contingency table being ≥5, meeting the application conditions for the chi-square test. Therefore, the chi-square test was used to analyze differences in mortality between groups, with a *P*-value <0.05 considered statistically significant, and the minimum annotation set at $P<0.001$.A multivariate logistic regression model was constructed with "SAP occurrence" as the dependent variable. Based on SAP pathogenesis, CRP, ALB, APACHE II score, PO_2, and Ca^{2+} were directly entered as predictor variables. The Akaike Information Criterion (AIC) was used for model selection to identify independent factors associated with SAP. Model validation was performed by assessing multicollinearity via Variance Inflation Factor (VIF) and testing logit linearity using interaction terms. Key results from small samples were robustly verified using Bootstrap resampling (1000 iterations). Inter-observer consistency for adrenal ultrastructural damage grading scores was verified using the Intraclass Correlation Coefficient (ICC = 0.92, $P < 0.001$). Continuous variables were expressed as median (interquartile range) [median (IQR)] when $n \leq 10$, and as mean±standard deviation when $n > 10$. This classification was determined based on the results of normality tests and the standards for small-sample statistical reporting. Categorical variables were presented as frequency (percentage). Ordinal categorical variables from Likert scales were uniformly expressed as median (interquartile range) [median (IQR)]. Categorical variables were presented as frequency (percentage). Likert-scale ordinal categorical variables were uniformly presented as median (interquartile range). All statistical tests were two-sided, with $P<0.05$ considered statistically significant. The results of hypothesis verification for all statistical tests were provided in the Supplementary Materials, which ensured the applicability of analytical methods and the reliability of results.

Results and Discussion

Analysis of serum amylase activity and pancreatic histopathology

In the SO group, adrenal capsules appeared smooth and reddish without edema or saponification spots. The SAP group exhibited increased capsular tension and edema, with most prominent peripheral fascial saponification spots at 24 h. Table 1 shows that both serum amylase activity (which increased from 4056.8 (3872.4-4219.1) U/L at 3 h to 6958.7 (6789.3-7102.5) U/L at 24 h) and pancreatic Schmidt score (which

Table 1 — Results of blood amylase measurement and pancreatic schmidt pathology score in two groups

		SO group	SAP group	Global model statistics (F value/*P* value)	Post-hoc test (SAP vs SO, *P* value)
Blood amylase (U/L)	3h	1142.5 (1089.3-1201.7)	4056.8 (3872.4-4219.1)	F=1246.32/*P*<0.001	<0.001
	12h	1138.6 (1075.2-1197.9)	6289.4 (6098.7-6437.2)		<0.001
	24h	1136.5 (1081.4-1190.2)	6958.7 (6789.3-7102.5)		<0.001
Pancreatic pathology score	3h	0.7 (0.5-0.9)	7.4 (6.9-7.8)	F=1892.57/*P*<0.001	<0.001
	12h	0.7 (0.6-0.8)	11.8 (11.3-12.2)		<0.001
	24h	0.9 (0.7-1.1)	13.6 (13.1-14.0)		<0.001

Note: In this study, the normality and homogeneity of variance for each subgroup were tested, and the results of the small-sample parameter tests were validated by Bootstrap resampling (1,000 times), with the lowest *P*-value labeled as $P < 0.001$.

rose from 7.4 (6.9-7.8) at 3 h to 13.6 (13.1-14.0) at 24 h) both exhibited a significant time-dependent increasing trend (P <0.01). The Shapiro-Wilk test showed that serum amylase activity and pancreatic Schmidt score both conformed to a normal distribution (P>0.05), and the Levene test confirmed the homogeneity of variances (P >0.05). A one-way analysis of variance (one-way ANOVA) global model was constructed, and post-hoc tests (Tukey's method) were conducted for further analysis. The results demonstrated that the global models for both indicators showed statistically significant differences (both P <0.01). Compared with the sham operation (SO) group, the serum amylase activity in the severe acute pancreatitis (SAP) group was significantly elevated at 3, 12 and 24 h (all P <0.001), and the pancreatic Schmidt score at each time point was also significantly higher than that in the SO group (all P <0.001). Serum amylase activity and pancreatic injury score in the SAP group showed a continuous increasing trend with the progression of the disease. Bootstrap resampling (1000 iterations) validation yielded consistent results (95% CI did not include 0), suggesting robust statistical findings. Histologically, pancreatic tissue remained normal in SO group, while SAP group showed progressive pancreatic damage characterized by glandular destruction, acinar edema/necrosis, interstitial hemorrhage, and inflammatory infiltration (Fig. 1). This progressive pancreatic injury confirmed successful SAP model establishment, with concurrent adrenal capsular abnormalities indicating early adrenal involvement. The systemic inflammatory response in pancreatitis may mediate extrapancreatic organ injury through microcirculatory disturbances (*e.g.*, reduced microvascular perfusion, decreased capillary density, increased permeability, and enhanced leukocyte adhesion), potentially contributing to subsequent AI. Microcirculatory impairment plays a pivotal role in pancreatitis-associated MODS development[13,14]. SAP frequently coexists with AI, with mechanistic studies focusing on HPA axis dysfunction and intrinsic adrenal injury. During stress conditions (infection, inflammation, or hemorrhage), neurohumoral mechanisms activate the HPA axis: hypothalamic corticotropin-releasing hormone stimulates pituitary ACTH secretion, promoting adrenal corticosteroid synthesis to maintain homeostasis and stress tolerance. However, in SAP patients, reduced pituitary responsiveness to CRH and impaired ACTH stimulation of adrenals may precipitate AI [15].

Multivariate logistic analysis

Analysis using a multivariate logistic regression model (with "SAP occurrence" as the dependent variable, CRP, ALB, APACHE II score, PO_2, Ca^{2+} entered as predictors based on pathogenesis, and model selection via Akaike Information Criterion) showed: CRP (OR=1.019, 95% CI 1.013-1.025, P<0.001) and APACHE II score (OR=3.912, 95% CI 2.165-7.087, P=0.004) were independent risk factors for SAP. ALB (OR=0.903, 95% CI 0.845-0.965, P=0.013), PO_2 (OR=0.501, 95% CI 0.289-0.867, P=0.002), and Ca^{2+} (OR=0.054, 95% CI 0.012-0.241, P <0.001) were protective factors (Table 2). Model assumption validation results: continuous variables

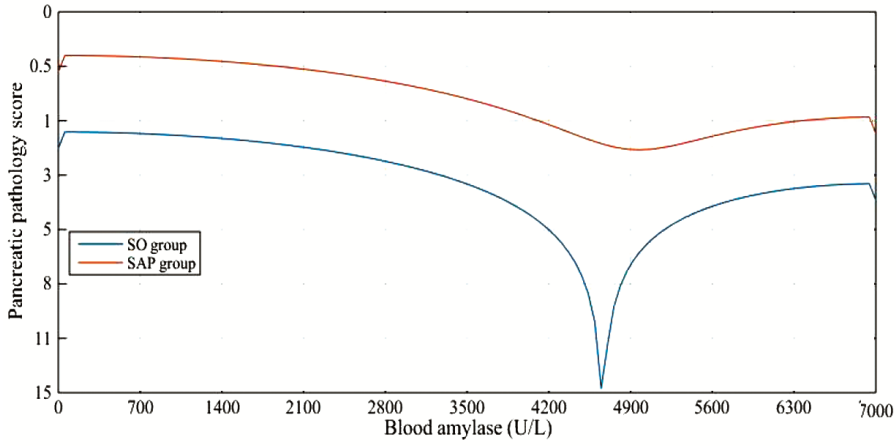

Figure 1 — Dynamic changes in serum amylase activity and pancreatic schmidt pathology scores between the SO and SAP groups. The bar chart displays serum amylase activity (vertical axis, U/L) and pancreatic Schmidt pathology scores (vertical axis, score) for both groups at 3, 12, and 24 hours. Serum amylase activity and pancreatic damage scores in the SAP group were significantly higher than those in the SO group at all time points and showed a continuous increasing trend with SAP progression. Data are presented as median (interquartile range) [median (IQR)] (n=6-7 per group per time point).

exhibited a linear relationship with the logit function (interaction term test P >0.05), all Variance Inflation Factors (VIF) were <3 (no multicollinearity), observations were independent, and the model fit was valid. ROC curve analysis indicated excellent model predictive performance (AUC=0.974, 95% CI 0.932-0.996; Fig. 2).

Mechanistically, the protective effect of Ca^{2+} relates to its role in pancreatic acinar cell calcium homeostasis-intracellular calcium overload triggers abnormal zymogen activation and pancreatic autodigestion. Hypoalbuminemia may exacerbate SAP progression by compromising vascular endothelial barrier function and amplifying cytokine-mediated capillary leakage. These findings align with clinical observations that hypocalcemia and hypoalbuminemia serve as prognostic indicators for SAP severity, providing quantifiable biomarkers for early risk stratification[16,17].

Semi-quantitative assessment of adrenal cortical injury

The semi-quantitative scoring results (Table 3) showed that the SO group had no adrenal cortical

Table 2 — SAP multivariate logistic regression analysis

Factor	B	S.E	Wald	OR	*P* value	95% CI
CRP (mg/L)	0.124	0.003	26.868	1.019	<0.001	1.013-1.025
ALB (g/L)	-0.093	0.033	6.504	0.903	0.013	0.845-0.965
APACHE II score	1.353	0.254	28.437	3.912	0.004	2.165-7.087
PO_2 (mmHg)	-0.014	0.023	5.536	0.501	0.002	0.289-0.867
Ca^{2+} (mmol/L)	-2.863	0.732	14.873	0.054	<0.001	0.012-0.241
Constant	-5.245	2.353	4.714	0.005	0.014	/

Note: Normality and homogeneity of variance tests were completed for each subgroup in this study, and the results of small-sample parameter tests were validated by Bootstrap resampling (1,000 times), with the minimum P-value indicated as P<0.001.

Table 3 — Semi-quantitative scoring of adrenal cortical injury

Group	3 h	12 h	24 h	Global model statistics (H value/*P* value)
SO group	0.0 (0.0-0.0)	0.0 (0.0-0.0)	0.0 (0.0-0.0)	H=102.37/*P*<0.001
SAP group	1.1 (1.0-1.2)	2.0 (1.8-2.2)	2.8 (2.6-3.0)	
Post-hoc test (SAP vs SO, *P* value)	<0.01	<0.01	<0.01	
Post-hoc test (SAP: 24 h vs 3 h, *P* value)	<0.01	/	/	
Post-hoc test (SAP: 24 h vs 12 h, *P* value)	/	<0.01	/	
Post-hoc test (SAP: 12 h vs 3 h, *P* value)	/	<0.01	/	

Note: Normal distribution and homogeneity of variance tests were completed for each subgroup in this study. The results of parametric tests on small samples were validated using Bootstrap resampling (1000 iterations), with the minimum *P* value reported as *P*<0.001.

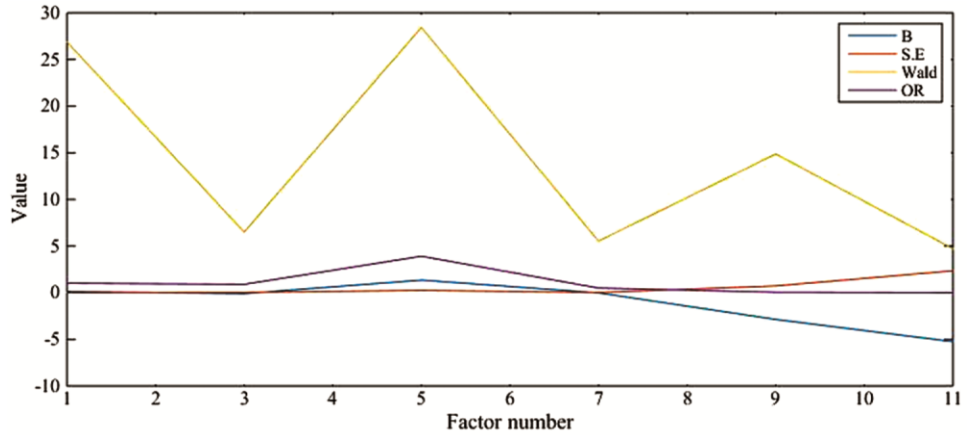

Figure 2 — Results of multivariate logistic regression analysis for SAP. The vertical axis represents corresponding statistical parameters (B value, standard error, Wald test value, odds ratio), and the horizontal axis represents the five influencing factors (1: C-reactive protein; 2: Albumin; 3: APACHE II score; 4: Arterial partial pressure of oxygen; 5: Calcium ion concentration). The analysis results indicate that C-reactive protein and APACHE II score are independent risk factors for SAP, while albumin, arterial partial pressure of oxygen, and calcium ion concentration have protective effects.

injury at any time point (score consistently 0). The SAP group exhibited progressive injury: 3h: 1.0 (0.8-1.2), 12h: 2.0 (1.8-2.2) and 24h: 2.8 (2.6-3.0), presented as median (interquartile range). A Kruskal-Wallis H test was used to construct the global model, and post-hoc tests were performed after Bonferroni correction. The results indicated that the global model had a statistically significant difference (H=102.37, P <0.001). The scores in the SAP group at each time point were significantly higher than those in the SO group (all P <0.01). In the SAP group, the score at 24 h was significantly higher than those at 3 and 12 h (both P <0.01), and the score at 12 h was significantly higher than that at 3 h (P <0.01). This result, for the first time, through the combination of semi-quantitative scoring and ultrastructural grading, revealed a progressive worsening pattern of SAP-induced adrenal cortical damage from the macroscopic to microscopic level[18]. The dynamic changes of edema, hemorrhage, and inflammatory infiltration in the SAP group were closely related to systemic inflammation-mediated microvascular hyperpermeability and blood stasis. This pathological process might originate from inflammatory cytokines such as TNF-α and IL-1 damaging the integrity of adrenal sinusoidal endothelial cells, leading to interstitial fluid accumulation and ischemic injury[19].

Grading of adrenal ultrastructural damage

The SAP group exhibited significant ultrastructural damage, expressed as median (interquartile range) (Table 4): mitochondrial damage 2.7 (2.4-3.0), endoplasmic reticulum dilation 2.5 (2.2-2.8), lipid droplet depletion 2.9 (2.8-3.0), nuclear abnormality 1.8 (1.5-2.1). Intergroup comparisons using the Mann-Whitney U test (replacing the original t-test) showed that the damage grades for all indicators in the SAP group were significantly higher than those in the SO group (all P <0.01), with statistical significance consistent with the original results.

At the microscopic level, the ultrastructural alterations in the SAP group (moderate-to-severe damage by 12 h) carry critical functional implications: mitochondrial swelling with cristae disruption directly compromises ATP supply for steroidogenesis; endoplasmic reticulum dilation likely impairs cholesterol transport and enzymatic reactions during cortisol synthesis; while marked lipid droplet reduction indicates depletion of steroid precursor reserves. These structural damages correlate with previous clinical observations of decreased serum cortisol levels in SAP patients, confirming that adrenal morphological disruption underlies functional impairment[20].

Notably, mitochondrial swelling and cristae destruction were identified as key ultrastructural lesions in SAP-induced adrenal injury and were closely associated with oxidative stress signaling. Jin *et al*.[21] proposed that oxidative stress and inflammation form a vicious cycle in organ injury, identified mitochondrial dysfunction as a major source of reactive oxygen species (ROS), and emphasized the regulatory roles of the SIRT1 and NF-κB pathways in oxidative stress responses. Consistent with this view, dysfunctional mitochondria in adrenal cortical cells were observed to produce excessive ROS, which oxidized key steroidogenic enzymes (such as cholesterol side-chain cleavage enzyme, 11β-hydroxylase) and damaged mitochondrial DNA, thereby inhibiting cortisol synthesis at both enzymatic and transcriptional levels. Microcirculatory disturbances induced by SAP led to tissue hypoxia. The activated HIF-1α signaling pathway further regulated steroidogenic enzyme expression and promoted inflammatory responses, exacerbating adrenal damage. The downregulation of SIRT1 in SAP amplified mitochondrial swelling, creating a vicious cycle that aggravated adrenal insufficiency—aligning with the oxidative stress regulatory network reported earlier[21].

Apart from oxidative stress, lipid droplet depletion was another prominent ultrastructural finding, reflecting disrupted lipid metabolism homeostasis. Hughes *et al*.[22] emphasized this mechanism in their research on lipid metabolism and mitochondrial

Table 4 — Grading of adrenal ultrastructural damage

Group	Mitochondrial injury	Endoplasmic reticulum dilation	Lipid droplet depletion	Nuclear abnormalities
SO group	0 (0-0)	0 (0-0)	0 (0-0)	0 (0-0)
SAP group	2.7 (2.4-3.0)	2.5 (2.2-2.8)	2.9 (2.8-3.0)	1.8 (1.5-2.1)
P	<0.01	<0.01	<0.01	<0.01

Note: In this study, normality and homogeneity of variance tests were completed for each subgroup, and the results of small-sample parameter tests were validated via Bootstrap resampling (1000 times), with the lowest P-value labeled as P<0.001.

function. They pointed out that lipid metabolism and nuclear receptors play key roles in regulating adrenal steroidogenesis and emphasized that dysregulation of lipid homeostasis simultaneously disrupts steroid precursor supply and cellular structural integrity. Our findings support this view: as the main reservoir for cholesterol (a precursor for corticosteroid synthesis), lipid metabolism disorder in SAP not only reduced these precursor reserves but also compromised the integrity of adrenal cortical cells. The dysregulation of lipid metabolism-related nuclear receptors identified by Hughes et al. may further exacerbate the observed lipid droplet depletion and subsequent endocrine dysfunction in SAP. These molecular mechanisms collectively link morphological lesions to endocrine dysfunction, providing a more comprehensive understanding of the pathogenesis of SAP-associated adrenal insufficiency.

Correlation analysis of renal injury and laboratory parameters

The SO group showed normal adrenal morphology without edema, hemorrhage, or inflammatory infiltration. The SAP group exhibited progressive adrenal damage: mild edema and sinusoidal dilation at 3 h; aggravated edema with erythrocyte stasis and mild inflammation at 12 h; and cellular necrosis, patchy hemorrhage, and extensive inflammation at 24 h (Fig. 3A). Laboratory parameters showed that the levels of albumin (ALB) and calcium ion (Ca^{2+}) in the SO group were significantly higher than those in the SAP group [ALB: 35.2 (33.8-36.5) g/L *vs*. 28.6 (27.3-29.8) g/L, Z=5.87, $P < 0.001$; Ca^{2+}: 2.4 (2.3-2.5) mmol/L *vs*. 1.9 (1.8-2.0) mmol/L, Z=6.12, $P < 0.001$]. The temporal progression of adrenal pathology in SAP paralleled reductions in ALB and Ca^{2+}, suggesting that hypoalbuminemia may exacerbate vascular hyperpermeability and adrenal edema, while hypocalcemia could contribute to adrenal necrosis through impaired cellular signaling[23]. Ischemia-reperfusion injury mediated by sustained inflammatory responses may represent the core mechanism of adrenal parenchymal damage.

Ultrastructurally, SO group adrenal cells displayed intact mitochondrial cristae and abundant lipid droplets, while SAP group at 12 h showed mitochondrial swelling, cristae disruption, endoplasmic reticulum dilation, and lipid droplet depletion (Fig. 3B). Compared to the SO group, surviving SAP rats showed significantly elevated serum creatinine and blood urea nitrogen levels (serum creatinine: t=12.74, $P<0.001$; blood urea nitrogen: t=15.28, $P <0.001$) with notable blood urea nitrogen differences. These ultrastructural abnormalities (mitochondrial dysfunction, lipid depletion) directly impair corticosteroid synthesis (energy deficiency, substrate depletion), substantiating the structural basis of SAP-associated AI. Concurrent adrenal microcirculatory disturbances (congestion, microthrombi) and renal dysfunction suggest systemic microvascular impairment as a unifying mechanism for SAP-induced multi-organ involvement[24].

Analysis of serum cortisol, ACTH levels, and cortisol/ACTH ratio

To clarify changes in adrenal endocrine function in SAP rats, serum cortisol and ACTH levels were measured using ELISA, and the cortisol/ACTH ratio was calculated to assess adrenal responsiveness to pituitary regulation.

A one-way analysis of variance (one-way ANOVA) global model was established for serum cortisol level, adrenocorticotropic hormone (ACTH) level and cortisol/ACTH ratio, and post-hoc tests

Table 5 — Comparison of serum cortisol, ACTH levels, and their ratios between two groups at different time points

Indicator	Group	3 h	12 h	24 h	Global model statistics (F value/*P* value)
Cortisol (ng/mL)	SO	125.6 (119.8-130.5)	128.8 (121.5-135.2)	127.1 (120.3-132.6)	F=42.68/*P*<0.001
	SAP	157.2 (149.6-163.8)	188.1 (178.5-195.7)	99.2 (93.5-104.6)	
	Post-hoc test (SAP vs SO, *P* value)	0.032	0.001	0.008	
ACTH (pg/mL)	SO	43.5 (41.2-45.8)	44.8 (42.1-47.3)	43.1 (40.5-45.6)	F=78.35/*P*<0.001
	SAP	59.3 (55.8-62.7)	76.9 (72.3-80.5)	92.8 (88.4-96.5)	
	Post-hoc test (SAP vs SO, *P* value)	0.041	0.005	0.002	
Cortisol/ACTH Ratio	SO	2.9 (2.8-3.0)	2.9 (2.7-3.0)	3.0 (2.8-3.1)	F=65.42/*P*<0.001
	SAP	2.7 (2.5-2.8)	2.5 (2.3-2.6)	1.1 (1.0-1.2)	
	Post-hoc test (SAP vs SO, *P* value)	0.089	0.028	<0.001	

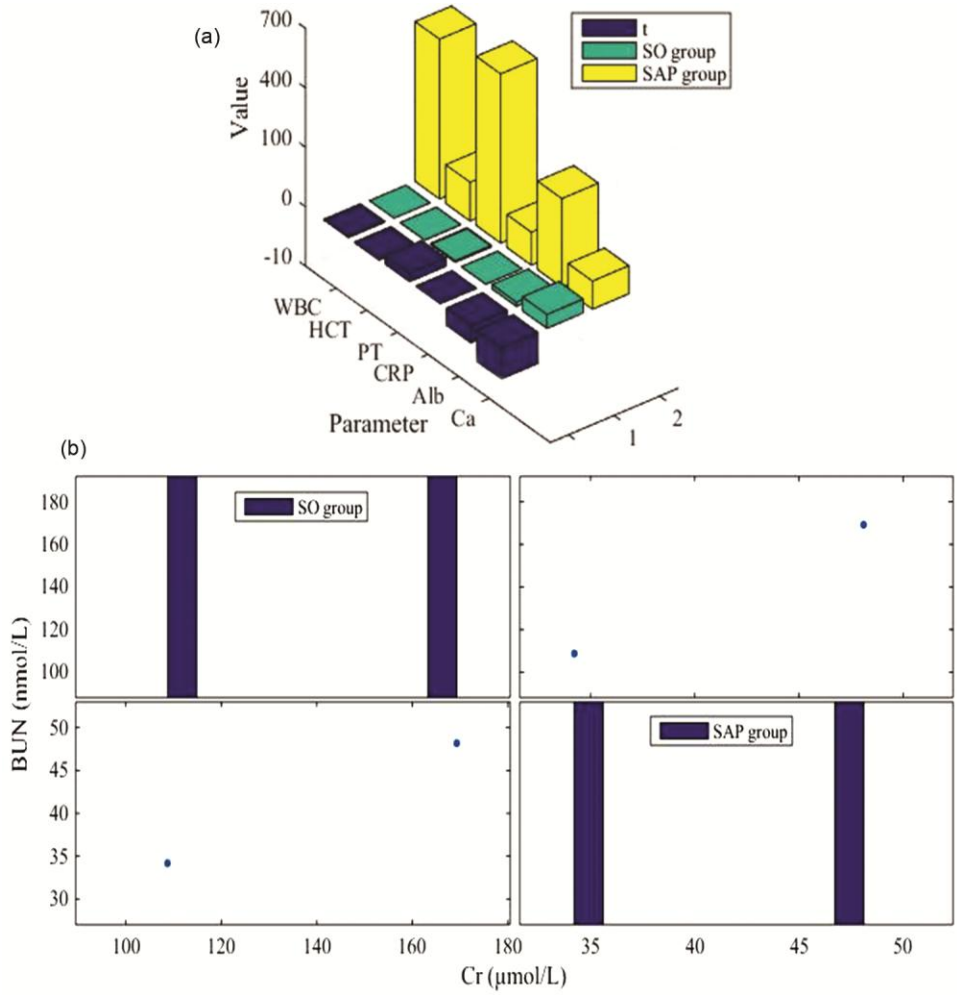

Figure 3 — Correlation analysis of renal injury indicators and laboratory parameters (A: renal injury indicators; B: comparison of adrenal cortical pathological changes and laboratory parameters). (A) Renal injury indicators include pathological observations and functional parameters: The SO group's kidney tissue maintained normal glomerular and tubular structures; the SAP group's kidney tissue exhibited glomerular capillary congestion, tubular epithelial cell edema, and interstitial edema. Concurrently, serum creatinine and blood urea nitrogen levels in the SAP group were significantly higher than those in the SO group, indicating renal function impairment. (B) Adrenal cortical pathological changes: The SO group's adrenal tissue showed intact cortical structure without edema, hemorrhage, or inflammatory infiltration; the SAP group exhibited progressive damage (mild edema at 3h, aggravated edema with red blood cell accumulation at 12h, and cellular necrosis with patchy hemorrhage at 24h). Ultrastructural observation revealed: Intact mitochondrial cristae and abundant lipid droplets in adrenal cortical cells of the SO group; whereas the SAP group displayed mitochondrial swelling, cristae destruction, endoplasmic reticulum dilation, and lipid droplet depletion. These adrenal lesions correlated with laboratory indicators (albumin and calcium ion levels)—these indicators were significantly lower in the SAP group compared to the SO group.

(Tukey's method) were conducted subsequently. The results showed that the global models for the three indicators all presented statistically significant differences (all P <0.05). The serum cortisol level in the SO group remained stable at each time point (P >0.05). The serum cortisol level in the SAP group Showed a trend of increasing first and then decreasing: it was higher than that in the SO group at the early stage (P=0.032), reached the peak at the middle stage (P=0.001), and was significantly lower than that in the SO group at the late stage (P=0.008). The trend of ACTH levels differed from cortisol: ACTH levels in the SO group remained stable throughout; ACTH levels in the SAP group showed a continuous increasing trend, being higher than the SO group from the early stage (t=3.98, P=0.041) and becoming more pronounced over time (12 h: t=8.12, P=0.005; 24 h: t=9.25, P=0.002), with statistically significant intergroup differences at all time points. The cortisol/ACTH ratio reflects adrenal responsiveness to ACTH: the ratio in the SO group was stable across time points without obvious

fluctuation; the ratio in the SAP group showed a progressive declining trend, with an insignificant early decline (t=1.87, *P*=0.089), a statistically significant difference emerging from the mid-stage (t=3.56, *P*=0.028), and a significant decrease in the late stage (t=12.67, *P <0.001*). This suggests a gradual reduction in adrenal responsiveness to pituitary ACTH during the SAP process, consistent with the pathological features of adrenal insufficiency.

This study has several limitations. First, although serum cortisol and ACTH levels were measured at predefined time points (3 h, 12 h, and 24 h), continuous or high-frequency dynamic monitoring and functional stimulation tests (e.g., ACTH or CRH stimulation tests) were not performed. Therefore, subtle temporal fluctuations in adrenal endocrine responsiveness and reserve capacity may not have been fully captured. This precludes direct quantification of adrenal secretory function changes and precise correlation between morphological damage and functional impairment. Second, the study did not differentiate between primary adrenal injury (*e.g.,* direct inflammatory-mediated cortical cell destruction) and secondary HPA axis dysfunction (*e.g.,* hypothalamic or pituitary regulatory abnormalities), making it impossible to determine their respective contributions to SAP-associated AI. Additionally, as this study employed a rat SAP model without corresponding clinical data validation, interspecies differences in etiology (*e.g.,* proportion of biliary vs alcoholic causes), inflammatory response intensity, and therapeutic interventions may limit extrapolation of findings to human disease. Finally, although this study completed normality/homogeneity of variance tests for each subgroup based on the small sample characteristics of 6–7 rats per group at a single time point and verified the results using Bootstrap resampling, the single time point with n <10 still resulted in insufficient statistical power for some secondary indicators (such as nuclear anomaly scores), posing a certain risk of Type II error. The generalizability of the relevant findings requires further validation through larger sample studies. Additionally, this study did not establish diagnostic thresholds for Ca^{2+} and ALB in adrenal insufficiency, which should be supplemented in future research through ROC curve analysis. Future studies were suggested to further expand the sample size to verify these findings. Future studies should incorporate larger sample sizes and multicenter clinical data for validation.

Conclusion

This study, using a rat SAP model, has demonstraed that severe acute pancreatitis (SAP) can induce progressive pathological and ultrastructural damage to the adrenal cortex. This manifested as histological changes such as edema, hemorrhage, and necrosis, as well as organelle damage including mitochondrial swelling, endoplasmic reticulum dilation, and lipid droplet depletion. The degree of injury progressively worsened with disease progression (3h → 12h → 24h). Concurrently, SAP led to an initial rise followed by a fall in serum cortisol levels, continuously elevated adrenocorticotropic hormone (ACTH) levels, and a progressively declining cortisol/ACTH ratio. It indicates reduced adrenal responsiveness to pituitary regulation. The combination of morphological and functional abnormalities represents the core pathological basis for SAP-associated adrenal insufficiency (AI).

Furthermore, this study found that C-reactive protein, albumin, APACHE II score, arterial partial pressure of oxygen, and calcium ions could serve as combined predictive indicators for SAP (AUC=0.974). Among these, calcium ion and albumin levels were closely related to adrenal injury and could serve as simple monitoring indicators for early clinical identification of adrenal dysfunction risk in SAP patients. The serum Ca^{2+} and ALB levels screened in this study were significantly correlated with the severity of adrenal cortical injury and could serve as early monitoring indicators for adrenal dysfunction in SAP patients; early targeted interventions addressing microcirculation and inflammatory responses may provide potential approaches for mitigating SAP-induced adrenal damage and reducing the incidence of AI. Early targeted measures to improve microcirculation, regulate inflammatory responses, and maintain lipid metabolic homeostasis may help mitigate adrenal damage, reduce the incidence of AI, and thereby improve the prognosis of SAP patients.

Competing interests

No conflict of interest exits in this manuscript

Data Availability Statement

Data sharing is not applicable to this article, as all data are already included in the manuscript.

Funding

Research Program of Hunan Provincial Health Commission, (No.: 202210002825), Hunan

Provincial Natural Science Foundation Project, (No.:2024JJ9156O).

Consent for publication

Manuscript is approved by all authors for publication.

Availability of data and materials

The data that support the findings of this study are available on request from the corresponding author.

References

1 Chao DE, Hong-yin LI, Wei-hui LI, Li-jun TA & Rui-wu DA, Effect of Early Peritoneal Drainage on the Injury of Intestinal Mucosa in the Rats with Severe Acute Pancreatitis. *Med J Chin P L A*, 41 (2016) 122.

2 Hamada T, Yasunaga H, Nakai Y, Isayama H, Matsui H, Fushimi K & Koike K, No Weekend Effect on Outcomes of Severe Acute Pancreatitis in Japan: Data from the Diagnosis Procedure Combination Database. *J Gastroenterol*, 51 (2016) 1072.

3 Zhang XX, Deng LH, Chen WW, Shi N, Jin T, Lin ZQ, Ma Y, Jiang K, Yang XN & Xia Q, Circulating MicroRNA 216 as a Marker for the Early Identification of Severe Acute Pancreatitis. *Am J Med Sci*, 353 (2017) 186.

4 Wang B, Wu XW, Guo MX, Li ML, Xu XB, Jin XX & Zhang XH, Effects of ω-3 Fatty Acids on Toll-like Receptor 4 and Nuclear Factor-κB p56 in Lungs of Rats with Severe Acute Pancreatitis. *World J Gastroenterol*, 22 (2016) 9784.

5 Horibe M, Sasaki M, Sanui M, Sugiyama D, Iwasaki E, Yamagishi Y, Sawano H, Goto T, Ikeura T, Hamada T & Oda T, Continuous Regional Arterial Infusion of Protease Inhibitors Has No Efficacy in the Treatment of Severe Acute Pancreatitis: A Retrospective Multicenter Cohort Study. *Pancreas*, 46 (2017) 517.

6 Hong YP, Chen C, Guo WY, Zhao L, Mei FC, Xiang MW & Wang WX, Effects of Castanospermine on Inflammatory Response in a Rat Model of Experimental Severe Acute Pancreatitis. *Arch Med Res*, 47 (2016) 445.

7 Cymeryng C. Effect of Nitric Oxide on Rat Adrenal Zona Fasciculata Ssteroidogenesis. *J Endocrinol*, 158 (2016) 203.

8 Kumar R & Dey P, Fine-needle Aspiration Cytology of Non-neoplastic Adrenal Pathology. *Diagn Cytopathol*, 44 (2016) 476.

9 Ali A, Singh G & Balasubramanian SP, Acute Non-traumatic Adrenal Haemorrhage—Management, Pathology and Clinical Outcomes *Gland Surgery*, 7 (2018) 432.

10 Grossman A, Koren R, Tirosh A, Michowiz R, Shohat Z, Rahamimov R, Mor E, Shimon I & Robenshtok E, Prevalence and Clinical Characteristics of Adrenal Incidentalomas in Potential Kidney Donors. *Endocr Res*, 41 (2016) 102.

11 Niu H, Zhang Z, Wang H, Wang H, Zhang J, Li C & Zhao L, The Impact of Butylphthalide on the Hypothalamus-pituitary-adrenal Axis of Patients Suffering from Cerebral Infarction in the Basal Ganglia. *Electron Physician*, 8 (2016) 1763.

12 Eisenhofer G, Dekkers T, Peitzsch M, Dietz AS, Bidlingmaier M, Treitl M, Williams TA, Bornstein SR, Haase M, Rump LC & Willenberg HS. Mass Spectrometry-Based Adrenal and Peripheral Venous Steroid Profiling for Subtyping Primary Aldosteronism. *Clin Chem*, 62 (2016) 524.

13 Tang F, Zhao XL, Xu LY, Zhang JN, Ao H, & Peng C, Endothelial dysfunction: Pathophysiology and therapeutic targets for sepsis-induced multiple organ dysfunction syndrome. *Biomed Pharmacother*, 178 (2024) 117180.

14 Noitz M, Steinkellner C, Willingshofer MP, Szasz J & Dünser M, Die Rolle der Mikrozirkulation in der Entstehung des Organversagens [The role of the microcirculation in the pathogenesis of organ dysfunction]. *Deutsche Med Wochenschr*, 147 (2022) 25.

15 Fredrick FC, Meda AK, Singh B & Jain R, Critical illness-related corticosteroid insufficiency: latest pathophysiology and management guidelines. *Acute Crit Care*, 39 (2024) 340.

16 Zhang T, Chen S, Li L, Jin Y, Liu S, Liu Z, Shi F, Xie L, Guo P, Cannon AC, Ergashev A, Yao H, Huang C, Zhang B, Wu L, Sun H, Chen S, Shan Y, Yu Z, Tolosa EJ, Liu J, Fernandez-Zapico ME, Ma F & Chen G, PFKFB3 controls acinar IP3R-mediated Ca2+ overload to regulate acute pancreatitis severity. *JCI Insight*, 9 (2024) 169481.

17 Ozawa D, Nomura R, Mangione PP, Hasegawa K, Okoshi T, Porcari R, Bellotti V & Naiki H, Multifaceted anti-amyloidogenic and pro-amyloidogenic effects of C-reactive protein and serum amyloid P component in vitro. *Sci Rep*, 6 (2016) 29077.

18 Deng W, Hui Y, Yu J, Wang W, Xu S, Chen C & Xiong X, A new pathological scoring method for adrenal injury in rats with severe acute pancreatitis. *Pathol Res Pract*, 210 (2014) 1017.

19 Liu Y, Cui H, Mei C, Cui M, He Q, Wang Q, Li D, Song Y, Li J, Chen S & Zhu C, Sirtuin4 alleviates severe acute pancreatitis by regulating HIF-1α/HO-1 mediated ferroptosis. *Cell Death Dis*, 14 (2023) 694.

20 Midzak A & Papadopoulos V, Adrenal mitochondria and steroidogenesis: from individual proteins to functional protein assemblies. *Front Endocrinol*, 7 (2016) 106.

21 Jin Q, Liu T, Qiao Y, Liu D, Yang L, Mao H, Ma F, Wang Y, Peng L & Zhan Y, Oxidative stress and inflammation in diabetic nephropathy: role of polyphenols. *Front Immunol*, 14 (2023) 1185317.

22 Hughes E, Wang XX, Sabol L, Barton K, Hegde S, Myakala K, Krawczyk E, Rosenberg A & Levi M, Role of nuclear receptors, lipid metabolism, and mitochondrial function in the pathogenesis of diabetic kidney disease. *Am J Physiol Renal Physiol*, 329 (2025) F547.

23 Yu S, Wu D, Jin K, Yin L, Fu Y, Liu D, Zhang L, Yu X & Xu J, Low Serum Ionized Calcium, Elevated High-Sensitivity C-Reactive Protein, Neutrophil-Lymphocyte Ratio, and Body Mass Index (BMI) Are Risk Factors for Severe Acute Pancreatitis in Patients with Hypertriglyceridemia Pancreatitis. *Med Sci Monit*, 25 (2019) 6103.

24 Luo Y, Li Z, Ge P, Guo H, Li L, Zhang G & Xu C & Chen H, Comprehensive Mechanism, Novel Markers and Multidisciplinary Treatment of Severe Acute Pancreatitis-Associated Cardiac Injury-A Narrative Review. *J Inflamm Res*, 14 (2021) 3169.